Earth Reinforcement, Ochiai, Yasufuku & Omine (eds) © 1996 Balkema, Rotterdam. ISBN 905410 833 9

Stability analysis of reinforced soil structures introducing some linear constraint conditions upon the 3-D velocity field

A. Asaoka
Nagoya University, Japan
G. Pokharel & T. Ochiai
Yahagi Construction Co., Ltd, Nagoya, Japan

ABSTRACT: A series of FE computations on reinforced soils were carried out introducing a new 3-D rigid plastic FE analysis method where a linear constraint condition of " *no-length change*" upon the consecutive soil nodes along a reinforcing bar are imposed. Stability of a reinforced soil slope was studied for varying friction angles and the reinforcement lengths. Axial force in the reinforcement, safety factor and velocity field were studied. The difference between the 2-D modeling of linear reinforcements as an equivalent continuous plate and linear reinforcements as is in 3-D analysis were distinguished. Effectiveness of the reinforcement in reducing the lateral deformation and improving the safety factor could be explained in better way than in the 2-D analysis. The 3-D analysis is more challenging and promising in studying the Reinforced Soil Structures and also to verify and improve the performance of the existing as well as newly proposed 2-D analysis methods e.g. RPFEM.

1. INTRODUCTION

The extensive use of reinforced soil technology in the present soil slope stability as well as embankment construction works has urged researchers to introduce most promising and precise methods for the computation of safety factor, axial force in the reinforcement, stress distribution in the soil mass and failure surface or failure modes of the reinforced soil structures. The FE methods introduced so far are still lagging in correctly modeling the mechanism of the reinforced soil system. Especially, the problem arises when the linear reinforcing bars are placed in staggered manner and spacing is not close enough to model the reinforcing bars as an equivalent continuous reinforcing plate just like in geogrod. The accuracy of computation, because of this assumption, decreases when ratio between the cross sectional area of the reinforcement to the circumferential area increases. The assumption of equal stiffness for the equivalent reinforcements in the 2-D FE analysis may over estimate the reinforcement-soil contact area, this. ultimately results the over-estimation of the shear force acting around the reinforcement which gives higher safety factor as well as higher reinforcement force. To overcome this problem, 3-D analysis becomes an essential so as to minimize the difference between the prediction versus performance of a structure once it is constructed. The fulcrum of the present research is to propose a new concept of computation for the reinforced soil structures when reinforcements are linear reinforcing bars, e.g. soil nails.

The reinforced soil system at limiting equilibrium state formulated by Asaoka et al.(1994) for 2-D analysis based on the rigid plastic finite element method (RPFEM) of Tamura et al.(1984,1987) is extended, in the present study, to the 3-D analysis of similar structures. In their formulation, a linear constraint condition which impose the length between two soil nodes along the reinforcement to remain constant during failure, called as " *no length change*" condition, is imposed upon the velocity field in the soil mass at limit state. The constraint condition is extended to the modeling of reinforcing bars in 3-D space. Based on this analysis procedure, factor of safety/failure load, the axial force in the reinforcement, mean confining pressure distribution in the soil mass and the velocity field of the reinforced soil mass at limiting equilibrium state are simultaneously computed.

The characteristics features of the proposed 3-D analysis method and effectiveness of the reinforcing bars in the soil mass are examined through analyzing a series of reinforced soil slopes with varying friction angles and reinforcement lengths. Advantages and limitations of the proposed methods are discussed in detail in reference to 2-D analysis methods.

2. MODELING OF REINFORCED SOILS

The formulation of "no-length change" are illustrated here in terms of the 3-D velocity field assuming that the soil mass is at limit state. This is just to incorporate this constraint condition into the rigid plastic finite element method in the perspective of 3-D analysis. The formulation is an extension from the 2-D analysis presented in the earlier paper(Asaoka et al.,1994).

1.1 *No-length Change Condition* in 3-D space

The concept of "no-length change" condition introduced by Asaoka et al.(1994) is explained here in the perspective of 3-dimensional problem which is almost similar to the one they introduced for the plane strain analysis. As discussed in the introduction, the linear reinforcing bars in 3-D space is modeled in 2-D plane strain modeling as a continuous plate. The third dimension in 3-D allows the reinforcements to behave as in real structures and the FE mesh discretization can exactly in this case can simulate the spacing of reinforcement on 3rd dimension.

Thus, the "no-length change" condition in 3-D space means the reinforcements in the soil mass fastens each soil elements touching the reinforcement along reinforcement axis. At the limit state of soil mass, the no-length change condition requires that every reinforcing lengths between two consecutive soil nodes remain constant. Referring Asaoka et al.(1994), the "no-length change" condition is mathematically derived based on $|\boldsymbol{l}| = |\boldsymbol{l}+\Delta\boldsymbol{l}|$, as shown in Fig. 1 where the plastic flow of A and B to A' and B', respectively, on a small time, dt is illustrated. The constraint condition can be simplified to the following linear equation.

$$(X_2 - X_1)^T(\dot{u}_2 - \dot{u}_1) = 0 \tag{1}$$

Above equation can be integrated for the total reinforced soil system by assembling each reinforcing elements in the matrix, C_t, in general form:

$$C_t\,\dot{\boldsymbol{u}} = \boldsymbol{0} \tag{2}$$

where $\dot{\boldsymbol{u}}$ is the vector of all nodal velocities. Considering AB (length $=l_1$) and BC (length $=l_2$) are reinforcing elements passing through A, B and C consecutive soil nodes along reinforcement axis, the assembled part of $C_t\dot{\boldsymbol{u}}=\boldsymbol{0}$ corresponding to these reinforcing elements AB and BC is in the following form:

$$\begin{bmatrix} \cdots & \cdots & \cdots & \cdots & \cdots \\ 0\ l_{1x}, l_{1y}, l_{1z}, -l_{1x}, -l_{1y}, -l_{1z} & 0, & 0, & 0, & 0 \\ 0\ 0, & 0, & 0, & l_{2x}, l_{2y}, l_{2z} & -l_{2x}, -l_{2y}, -l_{2z}\ 0 \\ \cdots & \cdots & \cdots & \cdots & \cdots \end{bmatrix} \{\dot{u}\} = \{0\} \tag{3}$$

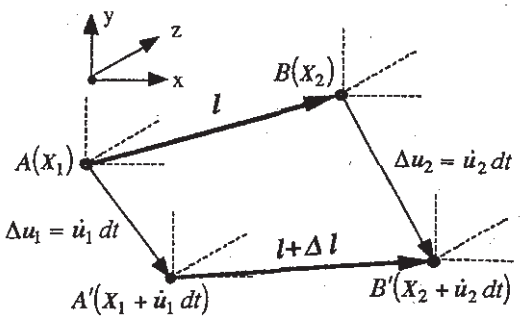

Fig.1 Concept of "*no-length change*"

where,

$$\dot{\boldsymbol{u}} = \left(.., \dot{u}_{Ax}, \dot{u}_{Ay}, \dot{u}_{Az}, \dot{u}_{Bx}, \dot{u}_{By}, \dot{u}_{Bz}, \dot{u}_{Cx}, \dot{u}_{Cy}, \dot{u}_{Cz}, ..\right)^T \tag{4}$$

3. INCORPORATION OF CONSTRAINT CONDITION INTO THE *RPFEM*

On the basis of the upper bound theorem on plasticity, the rigid plastic finite element method(RPFEM) is obtained through minimizing the rate of internal plastic energy dissipation with respect to the kinematically admissible velocity field under some linear constraint conditions (Tamura et al. 1984) as summarized in the next paragraphs.

The formulation is employed by introducing the Lagrange multipliers λ, μ, and υ to solve the minimization problem under constraint conditions. The following function is minimized:

$$\begin{aligned}\varphi(\dot{u}, \lambda, \upsilon, \mu) = {} & \int_V D(\dot{u})dV + \lambda^T(L\dot{u} - 0) \\ & + \upsilon^T(C_t\dot{u} - 0) + \mu\left(F^T\dot{u} - 1\right)\end{aligned} \tag{5}$$

in which $\boldsymbol{D}$ is the rate of internal plastic energy dissipation. L is the matrix defined such as $\dot{v} = L\dot{u}$ where $\dot{v}$ is the rate of volume changes in all elements. Therefore the first constraint condition, $L\dot{u} = 0$ indicates that rate of plastic volume change is always zero for all elements at the limit state (Mises material). The second constraint condition, $C_t\dot{u}=\boldsymbol{0}$ indicates the "*no length change*" condition, *see* Eq. (2). The third constraint condition, $F^T\dot{u}=1$ defines the provisional norms of velocity vectors at every node. As the rate of internal plastic energy dissipation, $D(\dot{u})$ is the convex function of $\dot{u}$, a local stationary condition of φ gives the global minimum of φ. Then taking the derivative of function, φ, one has the following equilibrium equation of forces at limit state and accompanied constraint conditions.

$$\int_V B^T s\, dV + L^T \lambda + C_t^T \upsilon + \mu F = 0 \quad (6)$$

$$L\dot{u} = 0 \quad (7)$$

$$C_t \dot{u} = 0 \quad (8)$$

$$F^T \dot{u} = 1 \quad (9)$$

in which s denotes the deviator stress vector while Lagrange multipliers λ and μ are interpreted as interpreted as the indeterminate isotropic stress and the load factor, respectively (Tamura et al., 1984). Interpretation of the Lagrange multiplier, υ, introduced to model the reinforcements is illustrated here.

The Lagrange multiplier, υ, is interpreted as the unit nodal forces acting on the constrained nodes along the reinforcement direction (Asaoka et al. 1994). For example, the forces calculated as υ in the horizontal reinforcement is illustrated in Fig. 2. The forth term in Eq. (6), $C_t^T \upsilon$, can be rewritten by the x, y component of the points A, B and C as follows:

$$C_t^T v = \left(l_{1x} v_1,\ 0,\ l_{2y},\ -l_{1x} v_1 + l_{2x} v_2,\ 0,\ -l_{2x} v_2,\ 0\right)^T \quad (10)$$

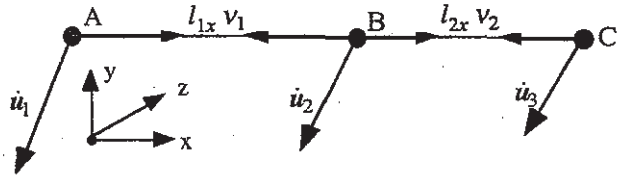

Fig. 2 Interpretation of υ as axial force per unit length along the reinforcement axis.

3.1 *Stress-Strain rate Relationships at Limiting Equilibrium State*

Eqs. (6)-(9) define statically indeterminate limiting equilibrium equation problems and these equations are solved with the aid of a constitutive relation of soils at limit equilibrium state. As the no rate of volume change is assumed in Eq. (7), the following the Mises type plastic flow is employed (Asaoka and Kodaka, 1994).

$$s_{ij} = \frac{\sigma_o}{\dot{e}} \dot{\varepsilon}_{ij} \quad \text{where} \quad \dot{\bar{e}} = \sqrt{\dot{\varepsilon}_{ij} \dot{\varepsilon}_{ij}} \quad (11)$$

where ε_{ij} denotes a plastic strain rate. In this study, the Mises constant σ_0 is assumed to follow non-dilatant Drucker Prager characteristics, that is,

$$\sigma_0 = \sqrt{2}(3\ \alpha\ p_m + k). \quad (12)$$

In plane strain matching, Drucker Prager constants are related to Mohr Coloumb constants as follows:

$$\alpha = \frac{\tan\phi}{\sqrt{\left(9 + 12\tan^2\phi\right)}},\quad k = \frac{3c}{\sqrt{\left(9 + 12\tan^2\phi\right)}} \quad (13)$$

in which p_m denotes the mean confining pressure and c and ϕ are the cohesion and frictional angle in Mohr-Coloumb type material under plane strain conditions, respectively. Note that the relationship of α and k with c and ϕ varies depends on the type of 3-D problem considered. The relationship mentioned in Eq.(12) is strictly applicable only under the plane strain conditions. In other words, Eqs.(12) define the Drucker-Prager type soil as an assembly of the inhomogeneous Mises materials(Fig.3) where each soil part consists of different σ_0 with respect to corresponding confining pressure, p_m,(Asaoka et al., 1994). Although this problem seem to follow the non-associated flow rule, the solutions obtained by iterative calculations satisfy the associate flow rule at the time of convergence, see the flow chart in Fig.4.

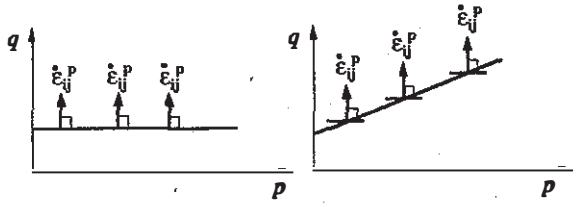

(a) purely cohesive clay (b) frictional soil

Fig.3 Modeling of non-dilatant soils

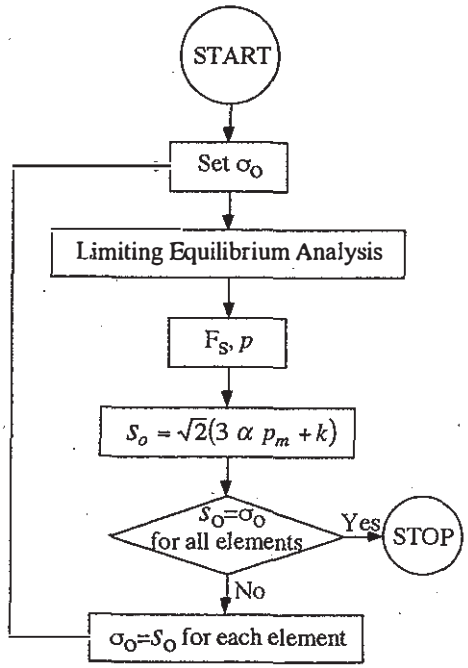

Fig.4 Flow chart adopted in the present 3-D analysis.

4. OUTLINE OF NUMERICAL ANALYSIS

The representative problem chosen is the stability analysis of slopes in which collapse is caused by the body force of soil mass and the slope is reinforced by a set of linear reinforcing material (e.g. steel bars/nails) inserted from the slope face like in soil nailing. The material constants for the Drucker Prager material are computed using Mohr Coloumb Parameters, c-ϕ, based on the plane strain matching as explained in the preceding sections. The case when α is zero, the Drucker Prager material is exactly same as the Mises material, i.e. purely cohesive clay.

In this study, the friction angle (ϕ) is increased from 0 to 25° at an interval of 5° to understand the effect of the frictional angle on the stability of reinforced soils, (i.e. safety factor and velocity field) and the axial force in the reinforcement.

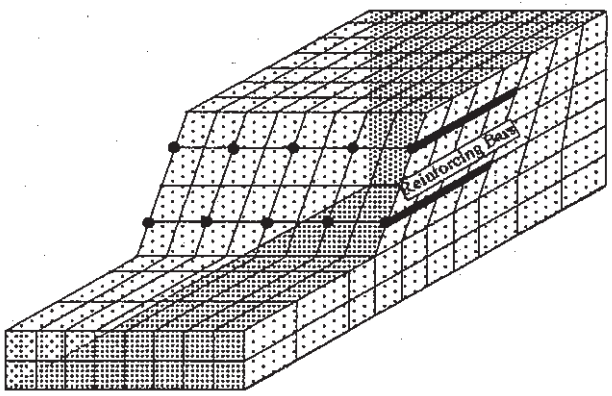

Fig.5 FE Arry for 3-D analysis[8].

Fig.5 shows the FE array and the boundary conditions used throughout this study. The height of the slope is kept 4 m and slope of the face is 1:0.5. The soil properties of the Mises material are c_u =10kN/m^2 and γ_t=18.4 kN/m^3. It should clearly noted here that the cross sectional area of the reinforcing material is not required at all because the reinforcing material is always assumed not to change length, in other words, the reinforcement is rigid in axial tension avoiding the need of absolute stiffness inside the numerical analysis.

Reinforcements are placed at different layers depending on the cases considered. There are especially 4 cases. Reinforcements are placed on each layers, i.e. 1.Top layer 2. Middle Layer and 3. Bottom Layer in individual cases and 4.Multiple Layer reinforced case where the Top and the Bottom Layers are reinforced at the same time. The reinforcements are laterally (in z-direction) are placed at 2 m spacing. Thus, in every alternative FE nodes in the lateral direction as shown in Fig. 5. The length of the reinforcement in all the cases mentioned above is fixed to 2m long. One additional set of computations are made for the middle layer reinforced with 4m long bar so as to illustrate the effect of reinforcement lengths. The computations for the unreinforced cases for different frictional angles, ϕ, are also presented for the comparison purposes.

5. RESULTS AND DISCUSSIONS

The numerical simulation work is performed, in the present study, using the rigid plastic finite element method (RPFEM) imposing the constraint conditions upon the 3-D velocity field as as introduced in the earlier sections. The RPFEM is used to compute the load factor for the gravity loading.

Figures 6 illustrates the variation of the safety factor with respect to the different friction angles. For illustration purposes, the velocity field in the soil mass and the axial force distribution in the reinforcing bars are presented, respectively in Figs. 7 and 8 where ϕ.=0°, 15°, and 25°. These figures present that the reinforcements are considerably effective in improving the stability of the soil mass and reducing the lateral deformation/plastic flow of the soil mass.

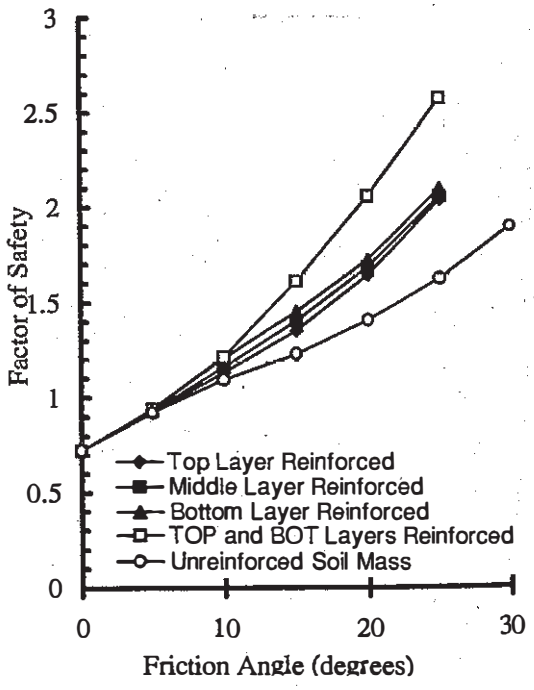

Fig.6 Variation of Safety Factor with ϕ for different bar positions (L_R=2m)

Velocity fields indicate wider failure zone for smaller friction angles and as the friction angle increases the failure zone approaches close to the slope face because of very low confining pressure near the slope face. Velocity vectors around reinforcements are normal to the reinforcement axis, thus, confirming the effectiveness of reinforcement in reducing the lateral flow of the soil mass.

Axial force in the middle layer and bottom layer reinforced cases have higher magnitudes compared to the axial force in the top layer reinforced case. Furthermore significant axial force developed at the inner side of the reinforcing bars in these cases can be clearly observed when the frictional angle becomes larger. In all the cases, the peak in the axial force distribution curve can be seen moving towards inner direction for larger friction angle because of high confining pressure around the inner end of the reinforcement. It indicates that the facing material if used, it confine the soil close to the slope face. The high confining pressure offered by the facing avoids the possibility of local failure close to the slope face.

Effect of reinforcement length can be visualized through the safety factor variation, velocity field, and axial force in the reinforcement shown in Fig.9. As the reinforcement length becomes very long, the reinforcement divides the velocity field into two clear failure zones up and under the reinforcement.

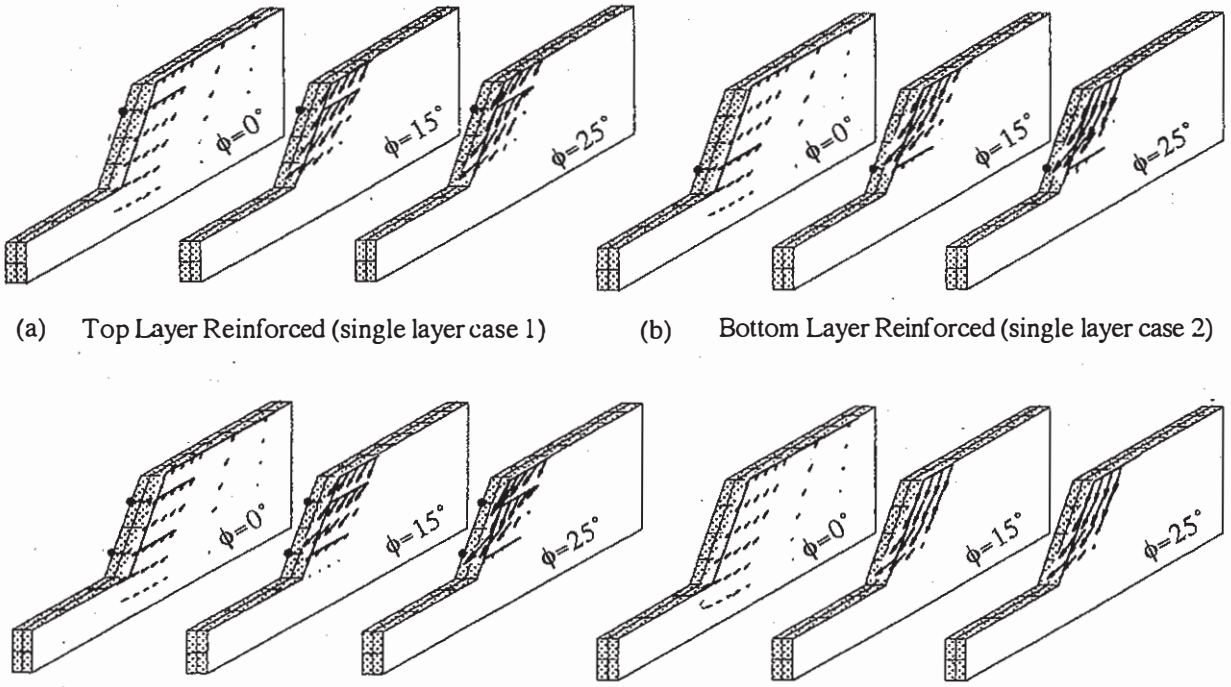

(a) Top Layer Reinforced (single layer case 1) (b) Bottom Layer Reinforced (single layer case 2)

(c) Top and Bottom (Multiple) Layers Reinforced (d) Unreinforced Soil Mass

Fig. 7 Velocity Field for different cases of reinforced cases and unreinforced soil mass

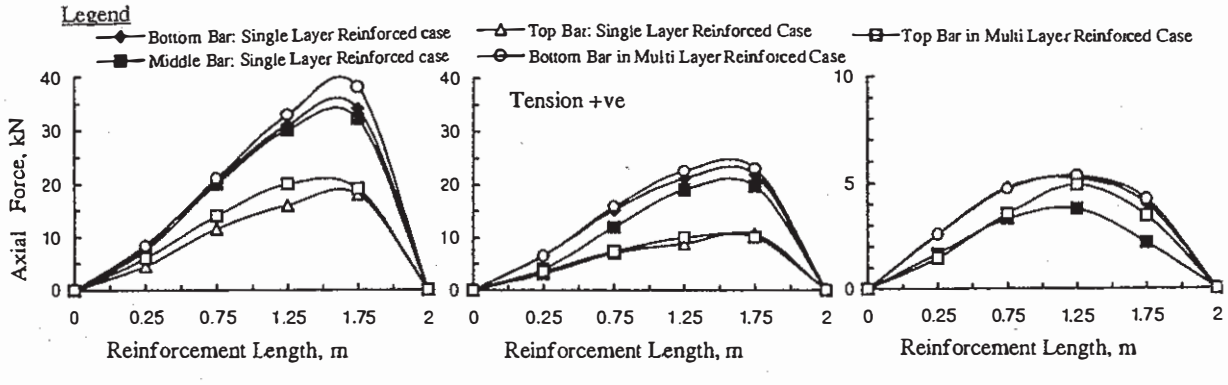

(a) ϕ=0° (b) ϕ=15° (c) ϕ=25°

Fig. 8 Axial Force in the reinforcement for different cases

Overall, the effect of modeling the linear reinforcements through 3-D FE analysis compared to the 2-D plane strain problem can be easily distinguished through the axial force distribution. The axial force in 2-D analysis assuming an equivalent continuous reinforcing plate is quite higher (Asaoka et al., 1994) than the 3-D analysis by modeling the linear reinforcement as it is in the real construction work. The higher factory of safety in 2-D RPFEM computations can be attributed to this difference in modeling the linear reinforcements. This should be the principle advantage of the 3-D analysis of the soil structures reinforced with linear reinforcing bars. Parametric studies through 3-D FE analysis may be carried out, to improve the performance of simplified 2-D analysis method. This should be the fulcrum of 3-D analysis.

6. CONCLUSIONS

A series of numerical computations on plain and reinforced soil slopes were presented. Behavior of these slopes were observed at the limit state of soil mass. In this study, the mechanism proposed by Asaoka et. al(1994) is extended to 3-dimensional analysis. Numerical computations were carried out based on the RPFEM. The following conclusions are drawn through the present study.

1). The mechanism of the reinforcement is modeled by employing the linear constraint condition of "*no-length change*" in energy functions. Performance of linear reinforcements is explained in 3-D analysis using the no length change condition, in better way than compared to the 2-D analysis when the reinforcements are linear reinforcing bars and not the continuous plates as assumed in arriving the 2-D plane strain condition. Therefore, the 3-D analysis should be used to evaluate the performance of simplified models in 2-D plane strain analysis and their further improvement.

2). The computed factor of safety is substantially increased when the soil mass is reinforced. The effect is more prominent as the friction angle increases. This confirms that the reinforcement is very effective in frictional soils as compared to the cohesive clays. It should be attributed to the very high confining pressure around the reinforcement.

3). Higher axial strain distributions in the reinforcements show that the efficiency of reinforcing bar increases as the frictional angle increases. The normal velocity vectors around reinforcements also confirms that the reinforcement is effective in reducing the lateral plastic flow of soil mass.

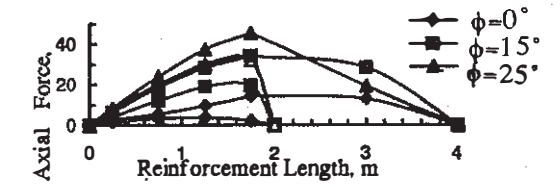

(a) Axial Force Distributions

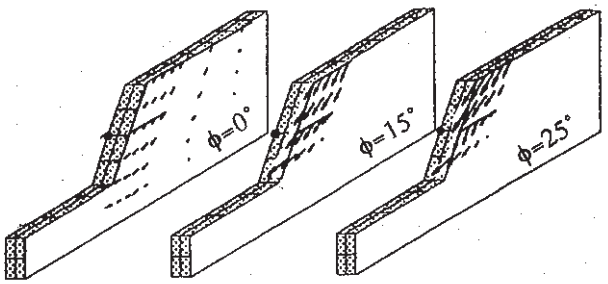

(b) Velocity Field for 2m Long Reinforcement

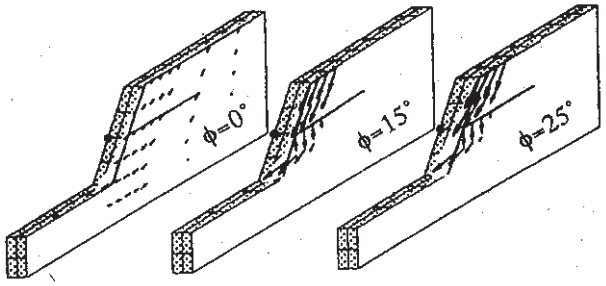

(c) Velocity Field for 4m Long Reinforcement

Fig. 9 Effect of Increasing Reinforcement Length (Middle Layer Reinforced Case)

REFERENCES

Asaoka, A., Kodaka, T. and Pokharel, G.(1994): Stability Analysis of Reinforced Soil Structures using Rigid Plastic Finite Element Method, Soils and Foundations, Vol. 34(1), p. 107-118.

Kodaka, T., Asaoka, A.and Pokharel, G.(1995): Model Tests and Theoretical Analysis of Reinforced Soil Slopes with Facing Panels, Soils and Foundations, Vol. 35(1), p. 133-145.

Pokharel, G.(1994): Deformation and Ultimate Load of Reinforced Soil Structures, D.Eng. Diss., Nagoya University, Japan, pp. 154.

Tamura, T., Kobayashi, S. and Sumi T.(1984): Limit Analysis of Soil Structure by Rigid Plastic Finite Element Method, Soils and Foundations, Vol. 24(1), p. 34-42.

Tamura, T., Kobayashi, S. and Sumi T.(1987): Rigid Plastic Finite Element Method for Frictional Material, Soils and Foundations, Vol. 27(3), p.1-12.